3D basin-scale groundwater flow modeling as a tool for geothermal prospection of the Geneva Basin, Switzerland-France

Alcanié M.[1] (marion.alcanie@unige.ch), Collignon M.[1], Møyner O.[2], Lupi M.[1],
[1] Earth and Environmental Sciences section, University of Geneva, Switzerland
[2] SINTEF Digital, Department of Mathematics & Cybernetics, Computational Geosciences group

1. Introduction and aims of the study

Switzerland supports the energetic transition by promoting the development of geothermal energy among other renewable energies. In particular, the Canton of Geneva is actively prospecting the Geneva Basin, generating a large dataset of geophysical and geological information.

Data catalog and previous studies

Previous studies described the geology of the Geneva basin [1]; [2]; [3]. The GeoMol project [4] more recently aimed at assessing the subsurface potentials of the Alpine Foreland Basins and Geothermie 2020 project are prospecting for geothermal exploitation. A large amount of data (wells and seismic lines) were acquired for hydrocarbon exploration. A review of the thousands of wells drilled in the Geneva area was done and helped characterized deep geothermal reservoirs [5] and provided geothermal gradient and thermal model [6]. Ca. 40 wells are fully documented, and only 3 in our study area reach layers deeper than the cretaceous (Fig. 1). The recent reprocessing of the 2D seismic lines added to new seismic campaigns allowed the definition of the main geological horizons geometry [7].

Numerical tool

In the frame of this project a geothermal module was developed as part of **MRST** (Matlab Reservoir Simulation Toolbox, [8]; [9]). We applied this code to build up a 3D basin-scale dynamic model of the Geneva Basin used as a natural laboratory. In a second time, MRST allowed us to rapidly prototype a parametric study and run several dynamic simulation.

Aims of study

- ▷ Understand the relation between local geology and fluid flow in the upper crust at the basin scale
- ▷ Investigate the large-scale control of tectonic structures and lithological heterogeneities on fluid flow
- ▷ Identify where promising areas for geothermal energy extraction within the Great Geneva Basin are located

2. Geological settings of the Great Geneva Basin

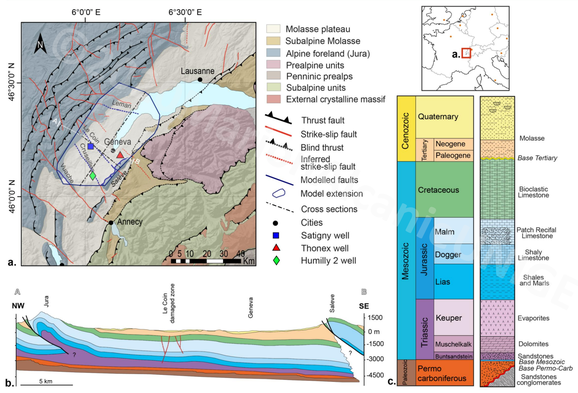

Figure 1.

a. Regional structural map of the Great Geneva Basin with the extension of the model and the location of the main faults and control points (well and cross-sections) considered in this study. Colored triangles: existing monitoring wells. White dashed lines: location of the cross-sections shown in Figures 2,3,5 and 7. Blue lines: modelled faults in our GGB model, with simplified geometric representation shown in Figure 2.

b. Vertical cross-section AB whose location is shown in Fig. 1a.

c. Simplified stratigraphic log of the GGB. Modified after [5]; [6]; [7].

3. Numerical model building

Geometric model

Model size: 40 by 35 km in the x- and y-directions (Fig. 2). Maximum elevation is about 1600m. Maximum depth is 5500m. Geometry is obtained from eight interpreted horizons to which the topography was added [4]; [7].

Meshing: with MRST using corner point geometry, Fixed number of cells per layer. The 3D model has 9 layers and a grid resolution of 100 by 100 by 45 cells.

Boundary and initial conditions

Simulation time: 500.000 years with 1000 steps of 500 years. No flow is prescribed at the lateral boundary. We consider the system laterally thermally insulated. We fix at the top boundary a constant pressure of 1 atm and a constant temperature T_{surf} of 10.3°C corresponding to the average annual temperature in the Geneva area. We do not apply bottom pressure conditions, and we consider a constant basal heat inflow of 73 mW.m^{-2} [6],[16]. The basin evolves without any external forces applied. The heat flux is hence representing the energy coming from the bottom part of the model and transferred only as heat conduction at initial state.

The initial pressure and temperature are computed using topography correction values. The pressure field is a simple hydrostatic pressure. The geothermal gradient is of 30,1 °C/Km from [6] with a surface temperature of 10.3°C to define our initial thermal conditions.

Rock Model Zero	Porosity	Permeability	Density	Thermal conductivity	Specific Heat capacity
	Φ (%)	m²	ρ (kg.m^{-3})	λ (W·m^{-1}·K^{-1})	Cp (J·kg^{-1}·K^{-1})
Quaternary Tertiary	0,107	6,519E-14	2400	2,6	1140
Cretaceous	0,015	7,106E-16	2670	3,0	928
Upper Malm	0,043	2,615E-16	2690	2,8	1021
Lower Malm	0,026	1,974E-16	2740	2,6	967
Dogger	0,028	8,241E-16	2650	2,8	972
Lias	0,023	7,234E-15	2640	2,6	935
Keuper	0,001	9,869E-19	2840	2,6	887
Musch. - Bunts.	0,033	1,382E-15	2740	2,9	923
Permo - carb.	0,033	1,382E-15	2710	2,9	887

Table 1. *Petrophysical values for the rock model 0*

Rock model

Petrophysical parameters were obtained from [4] and [5], for each layers between horizons (see lithology Fig. 3). For the model 0 (see Tab. 1), each layer has a constant permeability and porosity. Interpolation of the scarce well data is simply done by taking the mean value for a same layer. Thermal parameters are taken [5] or [6] when available, otherwise we applied a standard value from [12].

Fluid model

Pure water, compressible saturating the model. Density is set at 1000 kg.m^{-3} and viscosity to 1 mPa.s. They follow the equation of state defined in the MRST geothermal module [8]; [9]. Thermal fluid coefficient are chosen in the range of standard values [15]. Hence, thermal conductivity is 0.6 W·m^{-1}·K^{-1}, specific heat capacity is 4182 J·kg^{-1}·K^{-1}.

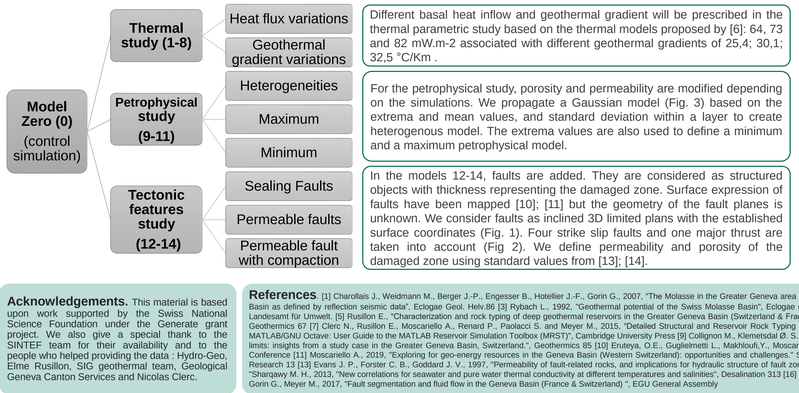

4. Results of the parametric study

4.1. Initial simulation : model zero

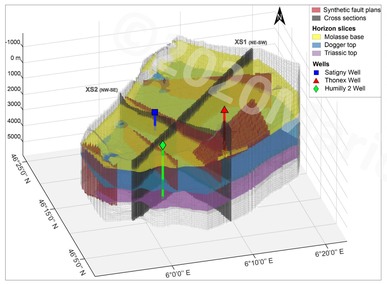

Figure 2.

3D geometric model with wells and faults, and two cross-sections used for monitoring in the next figures.

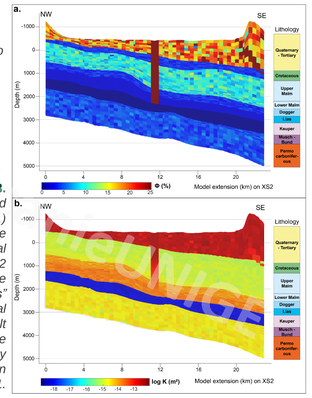

Figure 3.

Porosity (a.) and permeability (b.) distribution on the NW-SE vertical cross section (XS2 in Fig. 2) for the "heterogeneous" petrophysical model with fault (model 15). The modelled lithology displayed is shown in Fig.1.

Mathematical model

We consider a single-phase H2O compressible laminar flow in porous media. We solve the system describing the conservation of mass and energy using a fully implicit finite volume discretization with automatic differentiation and nonlinear solver implemented in MRST [8].
The geothermal module handles the complementary equations of state to the system [9].

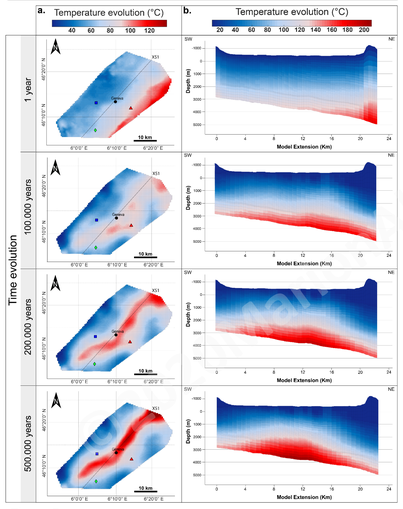

Figure 5.

Temporal evolution of the temperature at a. the top of the Dogger horizon and b. along XS2 (location on Fig. 2) for 500.000 simulated years for the model 0.

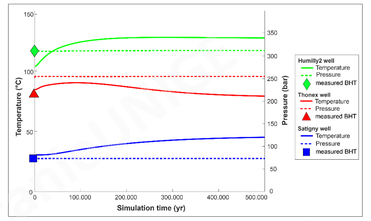

Figure 4.

Temporal evolution of the pressure (bar) and temperature (°C) at the three monitoring wells for the model 0.

- ► Steady state values are reached (Fig 4). Pressure does not differ much from initial state and rapidly equilibrates. The thermal re-equilibration is mostly linked to thermal conduction processes The temperature evolution presents a global slight warm up of the overall model.
- ► The difference between T_{BHT} at the control points and T_{MODEL} can be explained by the fact that the model 0 does not take into account the faults yet, and the thermal model used is not the most relevant to represent all the depths sections in the model [6].
- ► More rapid warm up in the basin central part than on the sides. This may be linked to a strong topographic effect over the basin.
- ► The highest temperatures for a horizon slice are found directly below the Leman lake which forms a warm anomaly plum.
- ► Darcian velocity show almost no flow in the center of the basin. Some small thermal convection cells in the first surface layer are observed with dipping flow up to 6 cm/year towards the deeper central basin part.

4.2. Effect of the permeability and porosity

- ► The heterogeneous model behaves more like the model with high porosities and permeabilities than the "minimum" model. With high permeability values, gravitational fluid transport is enhanced therefore warmer fluid goes up and cool down by thermal losses at the surface, resulting in a global cool down (increasing with depth) of the system and faster equilibrium.
- ► High variation amplitudes are observed in the model 11, with a cooling down of the central plum associated with a warming up of the rest of the model, for all the horizon slices. Due to very low permeability values, the fluid is not migrating and temperature equilibrium is not reached.
- ► A major impact of the topography is visible in every case, for the surface horizon, fading away at depth.
- ► The high temperature amplitude can be explained due to the insulation of the models and the high changes in petrophysical parameters driving to drastic modification. The impact of petrophysical parameters is twice more important in terms of variations than the thermal parameters.

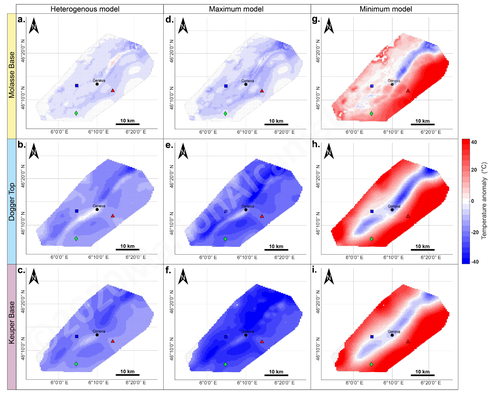

Figure 6.

Impact of the petrophysical variations on the temperature anomalies recorded after 500.000 simulated years for the "heterogeneous model" (a., b., c.), the "maximum" model (d., e., f.) and the "minimum" model (g., h., i.) with respect to the "model 0" (deltaT = Tpetro – T0). The three horizon slices "Molasse Base", "Dogger Top" and "Keuper Base" are shown in Fig. 2 and are displayed horizontally here.

4.3. Effect of the geothermal gradient and heat flow

- ► Scenarii from [6]: 25,4 °C/Km coupled with 82 mW.m-2 (Fig. 7c) and 30,1 °C/Km coupled with 64 mW.m-2 (Fig. 7d).
- ► The impact of the heat flux on the global temperature of the basin is higher than the geothermal gradient (one order of magnitude: 40 °C of amplitude compared to 4 °C respectively). A higher heat flux or geothermal gradient leads to a global increase of the model temperature. We also observe an increase of extremes values.
- ► Geothermal gradient has a higher impact at the first-time steps on temperature evolution that are eventually smoothed out when approaching steady state.

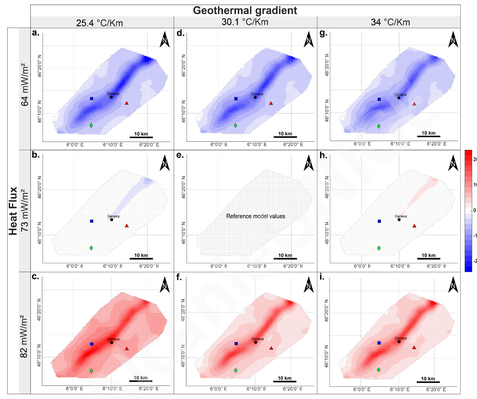

Figure 7.

Impact of the geothermal gradient (vertical) and heat flux (horizontal) on the temperature anomalies recorded at the Dogger top after 500.000 simulated years. Temperature anomalies are computed with respect to the model 0 (deltaT = Tfault – T0).

4.3. Effect of the tectonic features

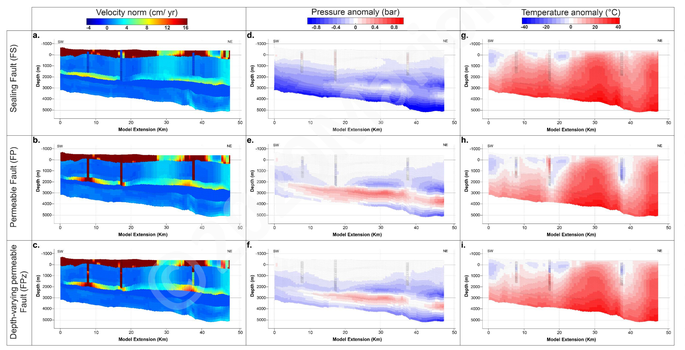

Figure 8.

Impact of different fault permeabilities on the velocity norm (a., b., c.), pressure anomalies (d., e., f.) and temperature anomalies (g., h., i.), recorded along XS1 (Fig.2). The three strike slip faults "Leman", "le Coin" and "Crusellles" are cross-cut by this section. Three permeability scenarios are considered: 1) sealed fault (top), permeable fault (middle) and depth-varying permeable fault (bottom). Pressure and temperature anomalies are computed with respect to the first-time step of the simulation (deltaT = Tfault(250.000) – Tfault(1) and deltaP = Pfault(500.000) – Pfault(1)). The velocity norm is obtained from the darcian flux vectors computed during the simulations after 500.000 years.

- ► The velocities are very lithology dependent; they naturally increase with higher permeabilities which make permeable faults automatic preferential flow paths (Fig. 8b, 8c) whereas sealing faults (Fig. 8a) have a closer behavior to the surrounding layer. Thermal convection cells are in place in the surface Molasse layer in every models showing downwarding and upwarding flows, but they are bypassed with the presence of permeable fault which show very high up-going velocities (20 to 30 cm/yr). The Dogger layer flow rates are very much increased by the presence of permeable fault.
- ► A small pressure drop starting from the bottom of the model is visible (Fig. 8d). When adding permeable faults (Fig. 8e, 8f) a slightly over-pressured layer is appearing located around the Keuper layer level. This is probably due to the evaporites level presenting very low porosity and permeability in the lithology model.
- ► The temperature anomalies display an overall increase of temperature with time for the three models. Constant high permeability with depth in the fault implies that the fluid will move up faster by buoyancy in this preferential channel. For a same depth, the surrounding of the fault will be colder, and at depth because of vertical migration the fluid will be found colder. The channeling features and central plum are strongly affected by faults crosscutting them in every models. The central warmer plum is deviated in every scenario toward the East under the Saleve mountain.

5. Applications, implications and limitations

Definition of the final model and results

Model 15 is built to be the most geologically representative of the GGB with average heat flux and geothermal gradient from [6] and [16]. We use the heterogeneous petrophysical model. Most faults are believed to be permeable after [17] so we keep the permeable fault model considering compaction.

A global cooling down (Fig.10) is mainly caused by the petrophysical heterogeneities. Even if the central part of the basin still shows the warmest temperatures, the shape of the plume is highly affected by the faults cross cutting it. Thermal convection (Fig. 9) is enhanced by the presence of faults in the Dogger permeable layer and in the Tertiary – Quaternary surface layer. The main fluid driver is the gravitational flow, probably linked to precipitation over the topographic highs.

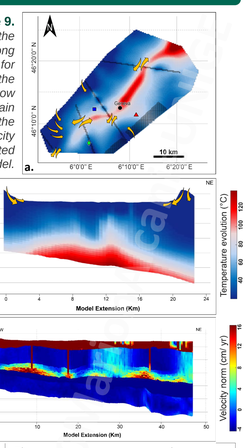

Figure 9.

Temperature at a. the top of the Dogger horizon and b. along XS2 (location on Fig. 2) for 500.000 simulated years for the final model. The yellow arrow are representing the main convection cells based on the darcian velocities maps. Velocity norm c. after 500.000 simulated years for the final model.

Comparison with other studies and implications

The thermal study done by [6] proposes a positive thermal anomaly around Humilly 2 well and at the Saleve ridge, potentially due to upward fluid circulation. This upward circulation is also visible at the fault in the vicinity of this well. The central warm plume visible here is not present on the previous study probably because of the use of different plotting scale.

Elevation maps of the main isotherms published in [4] shows that the 70 °C isotherm mainly follow the topography and is below 2000m depth in the centre of the basin which is consistent with our results. The side of our model differs much more, due to the side effects of the modeling.

The thermal state of the basin is not only simply based on conduction with fault permeabilities playing a major role in reaching any thermal state. We adopted here a dynamic approach which is complementing the previous static interpolation approaches done in the basin, and propose in-depth interpretations. The fault study provides a possible explanation for the observed artesian flow in the Satigny well.

Limitations and improvements

In the future, we consider adding some flow conditions for the regional and seasonal groundwater flow. The thermal insulation of the model at basin-scale may cause side effects artefact that should be investigated further.

We neglect the effect of salinity. The salinity measurements [5] are in average less than 10g/L which is three times lower than the mixtures usually characterized as brine. We do not consider any mechanical deformation, stress model or geochemical processes. The average low temperature in the Geneva Basin and relative depths allow for ignoring two phases flow. We assume petrophysical and hydraulic properties to be constant in time. Similarly, the boundary conditions maintain constant through time, due to a lack of recorded data.

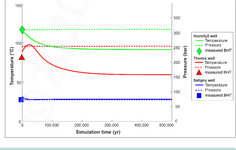

Figure 10.

Temporal evolution of the pressure (bar) and temperature (°C) at the three monitoring wells for the final model.

Acknowledgements. This material is based upon work supported by the Swiss National Science Foundation under the Generate grant project. We also give a special thank to the SINTEF team for their availability and to the people who helped providing the data : Hydro-Geo, Elme Rusillon, SIG geothermal team, Geological Geneva Canton Services and Nicolas Clerc.

References. [1] Charollais J., Weidmann M., Berger J.-P., Engesser B., Hotellier J.-F., Gorin G., 2007, "The Molasse in the Greater Geneva area and its substratum". Archives des Sciences, Société de Physique et d'Histoire Naturelle de Genève 60 [2] Gorin G.E., Signer C., Amberger G., 1993, "Structural configuration of the western Swiss Molasse Basin as defined by reflection seismic data", Eclogae Geol. Helv.86 [3] Rybach L., 1992, "Geothermal potential of the Swiss Molasse Basin", Eclogae geol. Helv. 85/3 [4] GeoMol Team, 2015, "GeoMol – Assessing subsurface potentials of the Alpine Foreland Basins for sustainable planning and use of natural resources – Project Report", Bayerisches Landesamt für Umwelt. [5] Rusillon E., "Characterization and rock typing of deep geothermal reservoirs in the Greater Geneva Basin (Switzerland & France)", PhD thesis: Univ. Genève, 2017 [6] Chelle-Michou C., Do Couto D., Moscariello A., Renard P., Rusillon E., 2017, "Geothermal state of the deep Western Alpine Molasse Basin,France-Switzerland", Geothermics 67 [7] Clerc N., Rusillon E., Moscariello A., Renard P., Paolacci S. and Meyer M., 2015, "Detailed Structural and Reservoir Rock Typing Characterization of the Greater Geneva Basin, Switzerland for Geothermal Resource Assessment", World Geothermal Congress 2015 [8] Lie K.-A., 2019, "An Introduction to Reservoir Simulation Using MATLAB/GNU Octave: User Guide to the MATLAB Reservoir Simulation Toolbox (MRST)", Cambridge University Press [9] Collignon M., Klemetsdal Ø. S., Møyner O., Alcanié M., Rinaldi A. P., Nilsen H. M., Lupi M., 2019, "Evaluating thermal losses and storage capacity in high temperature aquifer thermal energy storage (HT-ATES) systems with well operating limits: insights from a study case in the Greater Geneva Basin, Switzerland.", Geothermics 85 [10] Eruteya, O.E., Guglielmetti L., Makhloufi,Y., Moscariello A., 2019, "3-D Static Model to Characterize Geothermal Reservoirs for High-Temperature Aquifer Thermal Energy Storage (HT-ATES) in the Geneva Area, Switzerland", Poster SCCER-SoEAnnual Conference [11] Moscariello A., 2019, "Exploring for geo-energy resources in the Geneva Basin (Western Switzerland): opportunities and challenges." Swiss Bulletin für angewandte Geologie 24 [12] Waples D. W., Waples J. S., 2004, "A Review and Evaluation of Specific Heat Capacities of Rocks, Minerals, and Subsurface Fluids.", Natural Resources Research 13 [13] Evans J. P., Forster C. B., Goddard J. V., 1997, "Permeability of fault-related rocks, and implications for hydraulic structure of fault zones", Journal of Structural Geology 19 [14] Ingebritsen S. E., Manning C. E., 2010, "Permeability of the continental crust: dynamic variations inferred from seismicity and metamorphism". Geofluids 10 [15] "Sharqawy M. H., 2013, "New correlations for seawater and pure water thermal conductivity at different temperatures and salinities", Desalination 313 [16] Medici, F.; Rybach, L. Geothermal Map of Switzerland 1995; Commission Suisse de Géophysique [17] Cardello L., Lupi M., Makhlouli Y., Do Couto D., Clerci N., Sartori M., Samankassou E., Moscariello A., Gorin G., Meyer M., 2017, "Fault segmentation and fluid flow in the Geneva Basin (France & Switzerland) ", EGU General Assembly

Take home messages

- ► **Example of 3D basin-scale fluid flow modelling used as a preliminary prospection method for the assessment of geothermal resources. In this case, hotter fluids are found in the center of the basin where we propose to focus geothermal exploitation in the future**
- ► **Fluid flow is driven by the hydraulic head of the topographic highs bounding the basin. Permeable faults are the major preferential flow path and should be extensively studied in a next step**
- ► **First simplified petrophysical 3D model of the Geneva basin and first dynamic results.**